SINGLE UNDERWATER IMAGE DESCATTERING AND COLOR CORRECTION

Huimin Lu[*,#], *Yujie Li*[*], *Seiichi Serikawa*[*]

[*]Kyushu Institute of Technology, Japan
[#]Shanghai Jiaotong University, China

ABSTRACT

Absorption, scattering, and color distortion are three major issues in underwater optical imaging. Light rays traveling through water are scattered and absorbed according to their wavelength. Scattering is caused by large suspended particles that degrade optical images captured underwater. Color distortion occurs because different wavelengths are attenuated to different degrees in water; consequently, images of ambient underwater environments are dominated by a bluish tone. In the present paper, we propose a novel underwater imaging model that compensates for the attenuation discrepancy along the propagation path. In addition, we develop a fast weighted guided normalized convolution domain filtering algorithm for enhancing underwater optical images in shallow oceans. The enhanced images are characterized by a reduced noised level, better exposure in dark regions, and improved global contrast, by which the finest details and edges are enhanced significantly.

Index Terms— Underwater image, image enhancement, domain filter, spectral properties, wavelength compensation

1. INTRODUCTION

Following the recent development of autonomous underwater vehicles (AUVs), its application has been limited by issues in recognizing underwater objects. In the last two decades, sonars have been widely used for detecting and recognizing objects in underwater environments. However, for short-range identification, vision sensors must be used instead of sonars because sonars yield low-quality images [1].

In contrast to common photographs, underwater optical images suffer from poor visibility owing to the medium, which causes scattering, color distortion, and absorption. Large suspended particles cause scattering similar to the scattering of light in fog or turbid water that contain many suspended particles. Color distortion occurs because different wavelengths are attenuated to different degrees in water; consequently, images of ambient underwater environments are dominated by a bluish tone, because higher wavelengths are attenuated more quickly. Absorption of light in water substantially reduces its intensity. The random attenuation of light causes a hazy appearance as the light backscattered by water along the line of sight considerably degrades image contrast. In particular, objects at a distance of more than 10 m from the observation point are almost indistinguishable because colors are faded as characteristic wavelengths are filtered according to the distance traveled by light in water [2].

Many researchers have developed techniques to restore and enhance underwater images. Schechner et al. exploited a polarization filter to compensate for visibility degradation [3], while Bazeille et al. proposed an image pre-processing pipeline for enhancing images in turbidity water [4]. Fattal designed a graphic-theory-based independent-component analysis model to estimate the synthetic transmission and shading for recovering clean images [5]. He et al. estimated the dark channel prior through over 5000 nature images, then used soft matting to refine the depth map, and finally obtained clear images [6]. Nicholas et al. improved the dark channel prior and used the graph-cut method instead of soft matting to refine the depth map [7]. Hou et al. combined a point spread function and modulation transfer function to reduce the effects of blurring [8]. Ouyang et al. proposed bilateral filtering based on an image deconvolution method [9]. Ancuti et al. used an exposed fusion method in a turbid medium to reconstruct a clear image [10]. Chiang et al. considered the effects of variations in wavelength on underwater imaging and obtained the reconstructed image by using the dark channel prior model [11].

Although the aforementioned approaches can enhance the image contrast, they have several drawbacks that reduce their practical applicability. First, the imaging equipment is difficult to use in practice (e.g., a range-gated laser imaging system, which is rarely applied in practice [8, 9]). Second, multiple input images are required [3] (e.g., different polarization images or different exposed images) for fusing a high-quality image. Third, the image processing approaches are not suitable for underwater images [4, 6, 7] as they ignore the imaging environment, in addition to being time consuming. Fourth, too much manual operation is needed in processing, which leads to lack of intelligence [5].

In an underwater environment, the captured images are significantly influenced by inherent optical properties (e.g., wavelength, scatter, and absorption). Inspired by Chiang's work [11], in the present paper, we propose a novel shallow-ocean optical imaging model and a corresponding enhancement algorithm. We first estimate the depth map through dark channels. Second, considering the positions of the lighting lamp, camera, and imaging plane, we develop a rational imaging model. The effects of scattering are removed by using a weighted guided normalized convolution (WGNC) domain filter. Finally, color correction is performed by spectral properties. In our experiments conducted for verifying our proposed model and algorithm, we used a commercial RGB camera and natural underwater light. The performance of the proposed method is evaluated both analytically and experimentally.

2. UNDERWATER IMAGING MODELLING

Underwater imaging models generally follow a standard attenuation model to accommodate wavelength attenuation coefficients. In this paper the Koschmieder Model [12] is adopted which has been estimated as a description of the atmospheric effects of weather on the observer. However, for underwater imaging, the observed irradiance is linear combination attenuated in the route of sight and the scattered ambient light as depicted in Figure 1. Therefore, modified Koschmieder model has been adapted for underwater lighting conditions.

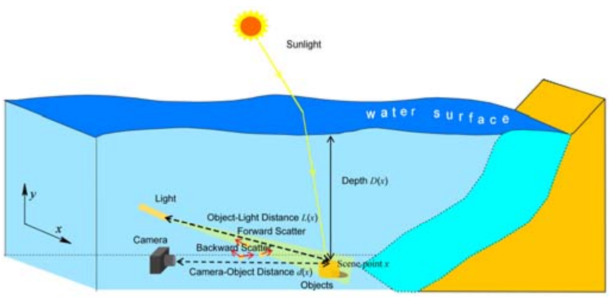

Fig. 1. Underwater Imaging Model. Light directly transmitted from the scene point *x* will be wavelength dependent exponentially attenuated over camera-object distance *d* and superimposed by the ambient illumination at depth *D*.

The modified Koschmieder model can be expressed as

$$I(x) = J(x)e^{-kd(x)} + \rho \cdot J(x)(1 - e^{-kd(x)}), \qquad (1)$$

where $J(x)$ is the real scene at depth $D(x)$, ρ is the normalized radiance of a scene point, d is the distance from the scene point to the camera and k is the total beam attenuation coefficient which is nonlinear and dependent on the wavelength.

The authors of [11] found that the red color channel is the dark channel of underwater images. During our experiments, we found that the lowest pixel value of the RGB channels in turbid water is not always the red color channel; the blue color channel is sometimes the lowest channel. This is usually caused by artificial light in imaging. Although light of red wavelength is easily absorbed when it propagates in water, the distance between the camera and object is not sufficient for light of red wavelength to be significantly absorbed. The blue channel is absorbed the least. Consequently, in this paper, we take the dual-channel (red and blue) value as a rough depth map.

Our method is based on [13], where the transmission is initialized using an underwater median dark channel prior (UMDCP). As mentioned before, we found that turbidly underwater images exhibited a mostly dark image $\tilde{d}(x)$ when the following morphological multiscale operator was applied to clear underwater images:

$$\tilde{d}(x) = \underset{\Omega(m,n)}{median}\left(\min_{\lambda \in \{r,b\}} \frac{I^{\lambda}(x)}{A^{\lambda}} \right) \qquad (2)$$

where Ω is a square window of sizes 5×5 or 7×7. For each pixel located at (m, n) of the square window Ω, the lower value from the red and blue color channels is chosen. The proposed method can prevent the halo effect around occlusion boundaries.

Accordingly, the coarse estimate of transmission is obtained by

$$\hat{d}(x) = 1 - \omega \tilde{d}(x) \qquad (3)$$

where $\omega = 0.98$ for most scenes.

3. PROPOSED METHOD

3.1. Weighted Guided Normalized Convolution Domain Filtering

In the previous subsection, we roughly estimated the camera–object distance $\hat{d}(x)$. However, its depth map contains mosaic effects and produces less accurate images. Therefore, we use a WGNC domain filter to reduce the mosaic effects. In this section, we introduce the constant time algorithm to develop the WGNC domain filter.

Use of the traditional median filter has been considered as an effective method for removing outliers. However, the traditional median filter usually leads to morphological artifacts such as rounded sharp corners. To address this problem, a weighted median filter [14] has been proposed. The weighted median filter is defined as

$$h(\mathbf{x}, i) = \sum_{\mathbf{y} \in N(\mathbf{x})} W(\mathbf{x}, \mathbf{y}) \delta(V(\mathbf{y}) - i), \qquad (4)$$

where $W(\mathbf{x}, \mathbf{y})$ corresponds to the weight assigned to a pixel $\mathbf{y}$ inside a local region centered at pixel x, the weight $W(\mathbf{x}, \mathbf{y})$ depends on the image d that can be different from V. $N(\mathbf{x})$ is a local window near pixel $\mathbf{x}$, i is the discrete bin index, and δ is the Dirac delta function.

Then, the refined depth map is computed using a weighted median filter with 2D normalized convolution domain transform filtering in the spatial domain as

$$h(\mathbf{x},i) = \sum_{\mathbf{y}\in N(\mathbf{x})} NC(\mathbf{x},\mathbf{y})\delta(V(\mathbf{y})-i), \quad (5)$$

where NC(x, y) is the 1D normalized convolution domain filter [15], which is defined as:

$$NC(\mathbf{x}) = (1/K_{\mathbf{x}}) \sum_{\mathbf{y}\in D(\Omega)} I_{NC}(\mathbf{y})H(t(\hat{\mathbf{x}}),t(\hat{\mathbf{y}})), \quad (6)$$

where $K_{\mathrm{x}} = \sum_{\mathrm{y}\in D(\Omega)} H(t(\hat{\mathrm{x}}),t(\hat{\mathrm{y}}))$ is a normalization factor for x, and $t(\hat{\mathrm{x}}) = t(x, ct(x))$. Using the efficient moving-average approach to apply NC with a box filter, the box kernel is

$$H(t(\hat{\mathbf{x}}),t(\hat{\mathbf{y}})) = \delta_B\{|\, t(\hat{\mathbf{x}}) - t(\hat{\mathbf{y}})\,| \le r\}, \quad (7)$$

where $r = \sigma_H\sqrt{3}$ is the filter radius, δ_B is a Boolean function that equals 1 when its argument is true and 0 otherwise, and σ_H is the standard deviation. The final refined depth map is produced by:

$$h(\tilde{d}(x),i) = \sum_{\mathbf{y}\in N(\mathbf{x})} NC(d(x),I)\delta(V(I)-i). \quad (8)$$

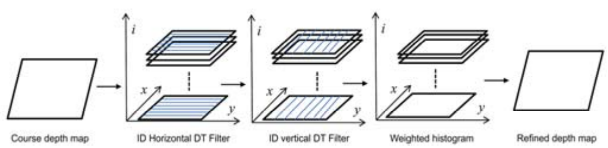

Fig. 2. Weighted normalized convolution domain filtering.

Figure 2 shows the pipeline of the weighted normalized convolution domain filter. The filter images, which preserve edges and filter noise on the basis of a dimensionality reduction strategy, have high quality while taking significantly less time compared to existing filters. The refined depth image is shown in Fig. 3.

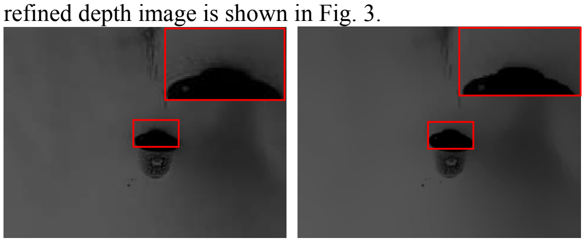

Fig.3. Depth map refinement using the weighted normalized convolution domain filter. (a) Input course depth image. (b) Refined depth image.

3.2. Color Correction

The authors of [11] simply corrected the scene color using the attenuation of light with respect to water depth. However, in practice, the spectral response function of a camera maps the relative sensitivity of the camera imaging system as a function of the wavelength of light. We use the chromatic transfer function τ for weighting the light from the surface to a given depth of objects as

$$\tau_\lambda = \frac{E_\lambda^{surface}}{E_\lambda^{object}}, \quad (9)$$

where the transfer function τ at wavelength λ is derived from the irradiance of the surface $E_\lambda^{surface}$ using the irradiance of the object E_λ^{object}. On the basis of the spectral response of the RGB camera, we convert the transfer function to the RGB domain:

$$\tau_{RGB} = \sum^{k} \tau_\lambda \cdot C_c(\lambda), \quad (10)$$

where τ_{RGB} is the weighted RGB transfer function, $C_c(\lambda)$ is the underwater spectral characteristic function for color band c, $c \in \{r,g,b\}$, and k is the number of discrete bands of the spectral characteristic function of the camera.

Finally, the corrected image is obtained from the weighted RGB transfer function using

$$J_\lambda(x) = \hat{J}_\lambda(x) \cdot \tau_{RGB}, \quad (11)$$

where $J_\lambda(x)$ and $\hat{J}_\lambda(x)$ are the color-corrected and uncorrected images, respectively.

4. RESULTS AND DISCUSSION

The performance of the proposed algorithm is evaluated both analytically and experimentally by utilizing ground-truth color patches. We also compare the proposed method with currently used state-of-the-art methods. The results reveal that the proposed method shows superior scattering removal and color balancing capabilities compared to other methods.

We tested our algorithm using simulations. Figure 4 shows the results, and Table 1 shows the quantitative analysis of the results. In the simulation, we took OLYMPUS Tough TG-2 underwater camera, the water depth $D(x)$ is 0.3 meters, and camera-object distance $d(x)$ is 0.8 meters. As a first step, we took the image in clean water and then, we captured the noisy image and added some turbid liquid in the tank. Size of the images is 640 × 480 pixels.

Figure 4 shows the results of using different de-scattering methods. Bazeille's pre-processing causes serious distortion. The drawback of Fattal's method is that the background and foreground in the image needs to be manually determined, and this is difficult in practical application. Nicholas's graph-cut-based method takes a lot of processing time, and the processed image is blurred. In comparison with He's method, our approach performs better because visible mosaic artifacts are observed in He's de-scattered image owing to the use of soft matting. In addition, there are some unresolved scatters around the object in Ancuti's model.

Chiang's de-scattered image has distorted colors.

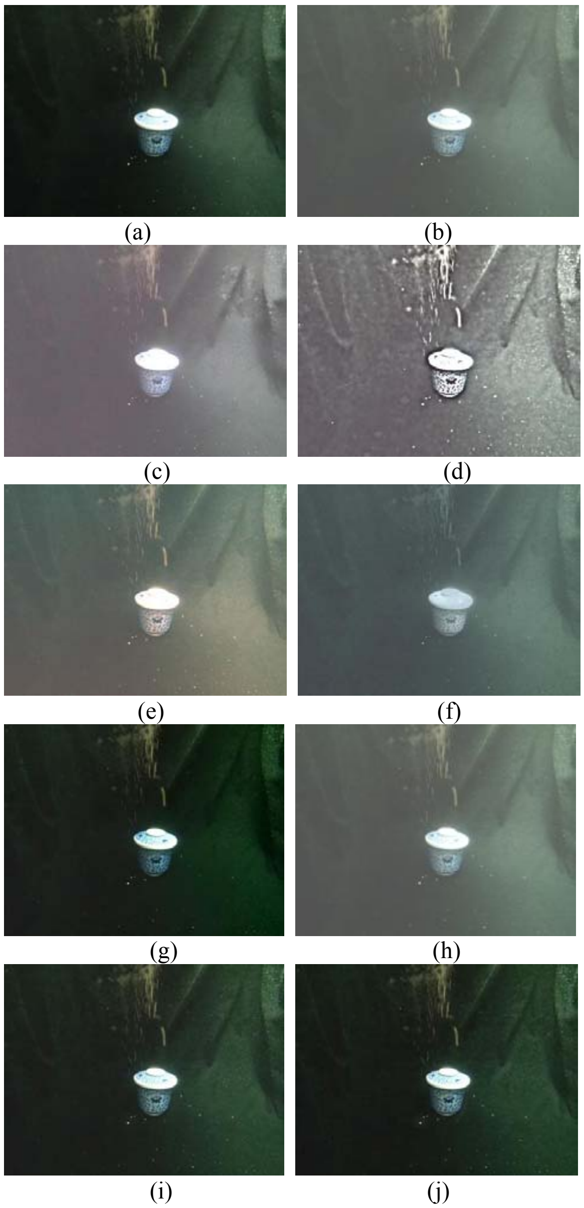

Fig.4. Simulation results of different descattering algorithms. (a) Noise-free image. (b) Noisy image. (c) Ancuti's result. (d) Bazeille's result. (e) Chiang's result. (f) Fattal's result. (g) He's result. (h) Nicholas's result. (i) Serikawa's result. (j) Our result.

The method proposed in our previous work [12, 18] performs well in de-scattering; however, it takes a lot of processing time, and the selection of parameters is difficult.

Table 1. Comparative Analysis of Different De-scattering Methods.

Methods	PSNR [dB]	Q-MOS	SSIM	CPU Time [s]
Ancuti	10.7715	30.8455	0.5530	30.15
Bazeille	9.5787	33.0082	0.4330	2.18
Chiang	11.7472	45.7409	0.5198	21.97
Fattal	13.9595	35.5432	0.6338	10.52
He	21.4046	40.6062	0.8534	37.45
Nicholas	12.4260	42.2650	0.5859	95.05
Serikawa	26.2365	63.7723	0.9204	4.61
The proposed	27.0520	71.1706	0.9266	4.01

In addition to the visual analysis, we conducted a quantitative analysis, primarily from the perspective of mathematical statistics and the statistical parameters of the images by MATLAB® (see Table 1). This analysis includes High-Dynamic Range Visual Difference Predictor2 (HDR-VDP2) [16], PSNR, and structural similarity index (SSIM) [17]. In HDR-VDP2, the Q-MOS value [16] is between 0 (best) and 100 (worst). Table I lists the Q-MOS values of the pixels filtered by applying HDR-VDP2-IQA in addition to SSIM values measured for several images. These results indicate that our approach not only works well for haze removal but also results in lower computation time.

5. CONCLUSION

In this study, we have explored and successfully implemented novel enhancement techniques for underwater optical images. We have proposed a simple prior based on the difference in attenuation among different color channels, which inspired us to estimate the transmission depth map. We introduced weighted guided normalized convolution domain filtering to compensate for transmission; this has benefits of preserving edges, removing noise, and reducing computation time. Moreover, the proposed underwater image colorization method successfully reconstructed colorful underwater images that are better than the images produced by state-of-the-art methods. Meanwhile, our method is faster by parallel algorithms in C++. Furthermore, our proposed method overcame the limitations due to the influence of artificial light sources. Our experiments showed that the proposed methods are suitable for underwater optical imaging.

6. ACKNOWLEDGEMENTS

This work was partially supported by Grant in Aid for JSPS Research Fellows (No.13J10713), Grant in Aid for JSPS International Research Fellows (No.P15077), State Laboratory of Ocean Engineering in Shanghai Jiaotong University, China (No.1315), and the Telecommunications Advancement Foundation.

7. REFERENCES

[1] D. M. Kocak, F. R. Dalglcish, F. M. Caimi, and Y. Y. Schechner, "A focus on recent developments and trends in underwater imaging," *Marine Technology Society Journal* 42(1), pp. 52–67, 2008.

[2] R. Schettini, S. Corchs, "Underwater image processing: state of the art of restoration and image enhancement methods," *EURASIP Journal on Advances in Signal Processing*, No.746052, 2010.

[3] Y. Y. Schechner, N. Karpel, "Recovery of underwater visibility and structure by polarization analysis," *IEEE Journal of Oceanic Engineering* 30(3), pp. 570–587, 2005.

[4] S. Bazeille, I. Quidu, L. Jaulin, J. P. Malkasse, "Automatic underwater image pre-processing," in Proc. of Caracterisation Du Milieu Marin (CMM '06), pp. 1–8, 2006.

[5] R. Fattal, "Single image dehazing," *ACM Transaction on Graphics* 27, pp. 1–8, 2008.

[6] K. He, J. Sun, X. Tang, "Single image haze removal using dark channel prior," *IEEE Transactions on Pattern Analysis and Machine Intelligence*, 33(12), pp. 2341–2353, 2011.

[7] C.-B Nicholas, M. Anush, R. M. Eustice, "Initial results in underwater single image dehazing," in Proc. of IEEE OCEANS, pp. 1–8, 2010.

[8] W. Hou, D. J. Gray, A. D. Weidemann, G. R. Fournier, and J. L. Forand, "Automated underwater image restoration and retrieval of related optical properties," in Proc. of IEEE International Symposium of Geoscience and Remote Sensing, pp. 1889–1892, 2007.

[9] B. Ouyang, F. R. Dalgleish, F. M. Caimi, A. K. Vuorenkoski, T. E. Giddings, and J. J. Shirron, "Image enhancement for underwater pulsed laser line scan imaging system," in Proc. of SPIE, 83720R, 2012.

[10] C. Ancuti, C. O. Ancuti, T. Haber, P. Bekaert, "Enhancing underwater images and videos by fusion," in Proc. of IEEE Conference on Computer Vision and Pattern Recognition, pp. 81–88, 2012.

[11] J. Y. Chiang, Y. C. Chen, "Underwater image enhancement by wavelength compensation and dehazing," *IEEE Transactions on Image Processing*, 21(4), pp. 1756–1769, 2012.

[12] H. Lu, Y. Li, S. Serikawa, "Underwater image enhancement using guided trigonometric bilateral filter and fast automation color correction," in Proc. of 20th IEEE International Conference on Image Processing, pp. 3412–3416, 2013.

[13] P.Drews-Jr, E.D. Nascimento, F. Moraes, S. Botelho, M. Campos, "Transmission estimation in underwater single images," in Proc. of ICCV Underwater Workshop, pp.825-830, 2013.

[14] L. Yin, R. Yang, M. Gabbouj, Y. Neuvo, "Weighted median filters: a tutorial," *IEEE Transactions on Circuits and Systems II*, 43(3). pp. 157–192, 1996.

[15] E. S. L. Gastal, M. M. Oliveira, "Domain transform for edge-aware image and video processing," *ACM Transactions on Graphics*, 30(4), pp. 1–8, 2011.

[16] R. Mantiuk, K. J. Kim, A. G. Rempel, W. Heidrich, "HDR-VDP2: a calibrated visual metric for visibility and quality predictions in all luminance conditions," *ACM Transactions on Graphics*, 30(4), pp. 40–52, 2011.

[17] Z. Wang, A. C. Bovik, H. R. Sheikh, E. P. Simoncelli, "Image quality assessment: From error visibility to structural similarity," IEEE Transactions on Image Processing, 13(4), pp. 600–612, 2004.

[18] S. Serikawa, H. Lu, "Underwater image dehazing using joint trilateral filter," *Computers & Electrical Engineering* 40(1), pp.41-50, 2014.